



**IAEA**

International Atomic Energy Agency

INDC(NDS)-0615

Distr. J+NM

## **INDC International Nuclear Data Committee**

### **Evaluation and compilation of neutron/proton-induced fission cross-sections for Hg, Pb, Bi, Th and U at 20MeV to 1 GeV**

IAEA Technical Report to Contractual Service Agreement

Prepared by

S. Yavshits

V.G. Khlopin Radium Institute, St. Petersburg, Russia

O.T. Grudzevich

Obninsk State Technical University, Obninsk, Russia

April 2012

Selected INDC documents may be downloaded in electronic form from  
<http://www-nds.iaea.org/reports-new/indc-reports/>

or sent as an e-mail attachment.

Requests for hardcopy or e-mail transmittal should be directed to  
[services@iaea.org](mailto:services@iaea.org)

or to:

Nuclear Data Section  
International Atomic Energy Agency  
Vienna International Centre  
PO Box 100  
1400 Vienna  
Austria

Printed by the IAEA in Austria

April 2012

**Evaluation and compilation of neutron/proton-induced fission cross-sections  
for Hg, Pb, Bi, Th and U at 20MeV to 1 GeV**

IAEA Technical Report to Contractual Service Agreement

Prepared by

S. Yavshits

V.G. Khlopin Radium Institute, St. Petersburg, Russia

O.T Grudzevich

Obninsk State Technical University, Obninsk, Russia

April 2012



## CONTENTS

1. Introduction.....	1
2. Evaluation approach .....	1
2.1 Entrance chanel .....	3
2.2 Intranuclear cascade .....	4
2.3 Preequilibrium multiparticle emission .....	4
2.4 Fission fragment formation .....	5
3. Comparison with experimental data and other evaluations and compilation of results ....	5
3.1 Comparison with experimental data and other evaluations .....	5
3.1.1 Fission cross-sections .....	5
3.1.2 Independent yields of fission fragments.....	13
3.2 Data compilation .....	27
3.2.1 Contents of KRITI library .....	27
3.2.2 Contents of KRIFF library .....	28
References .....	28











---

Nuclear Data Section  
International Atomic Energy Agency  
Vienna International Centre, P.O. Box 100  
A-1400 Vienna  
Austria

---

e-mail: [services@iaeand.iaea.org](mailto:services@iaeand.iaea.org)  
fax: (43-1) 26007  
telephone: (43-1) 2600-21710  
Web: <http://www-nds.iaea.org>

## CONTENTS

1. Introduction.....	1
2. Evaluation approach .....	1
2.1 Entrance chanel .....	3
2.2 Intranuclear cascade .....	4
2.3 Preequilibrium multiparticle emission .....	4
2.4 Fission fragment formation .....	5
3. Comparison with experimental data and other evaluations and compilation of results ....	5
3.1 Comparison with experimental data and other evaluations .....	5
3.1.1 Fission cross-sections .....	5
3.1.2 Independent yields of fission fragments.....	13
3.2 Data compilation .....	27
3.2.1 Contents of KRITI library .....	27
3.2.2 Contents of KRIFF library .....	28
References .....	28



**Evaluation and compilation of neutron/proton-induced fission cross-sections for Hg, Pb, Bi, Th and U at 20 MeV to 1 GeV.**

S.Yavshits

V.G.Khlopin Radium Institute, St.Petersburg, Russia; [yav@mail.rcom.ru](mailto:yav@mail.rcom.ru)

**1. Introduction**

The main goal of this work is to a nuclear data evaluation to meet needs of new nuclear technologies based on charged particle accelerators for energy production and radioactive waste transmutation.

The work plan consists of

1. Evaluation of neutron/proton-induced fission product yields and fission cross-sections for Hg, Pb, Bi, Th and U at 20 MeV to 1 GeV
2. Compilation of evaluated data to the ENDF-6 Format (INSUB=11/10011, MF-8, MT=454/459)
3. Comparison of evaluated data with available experimental data and other evaluated data.

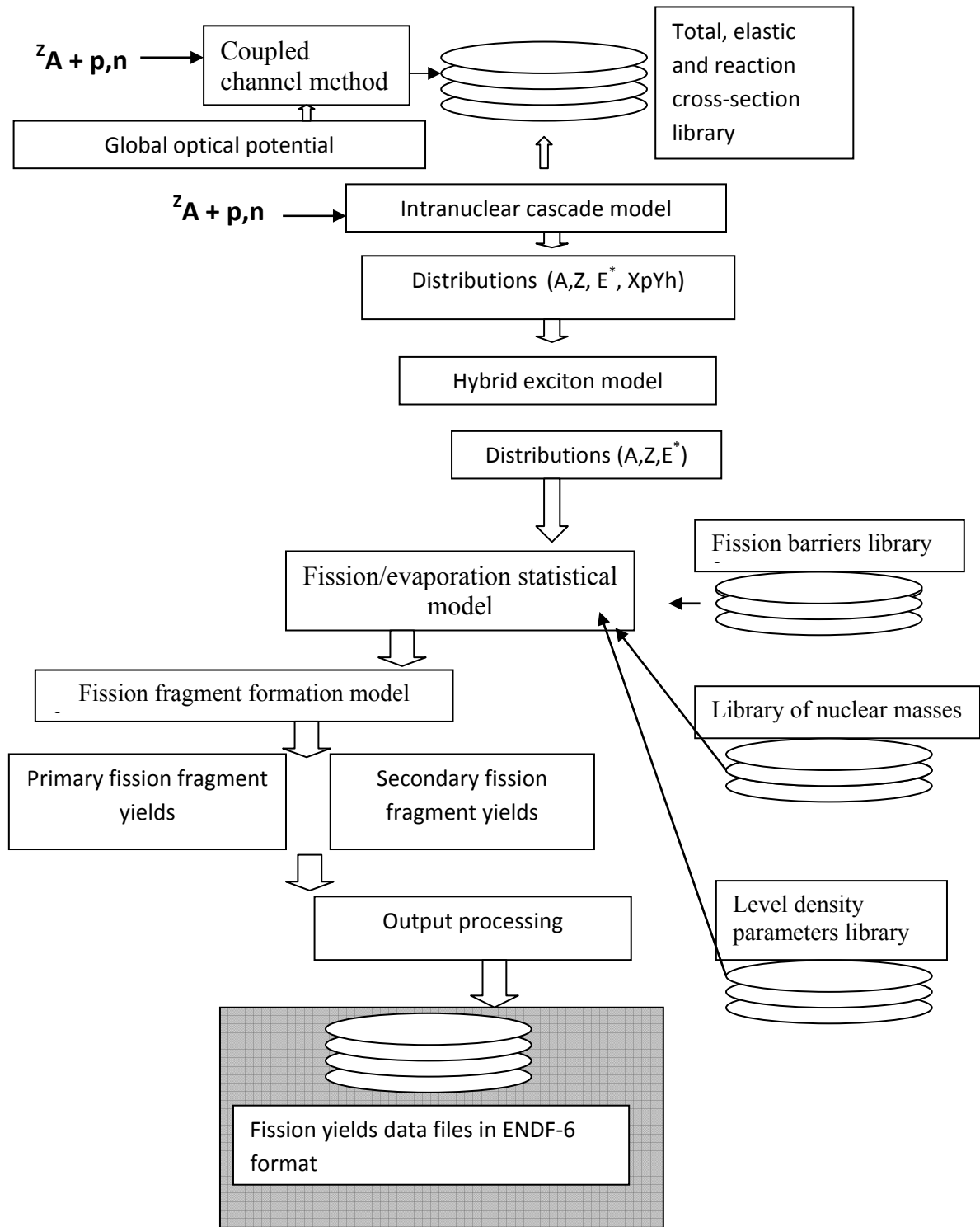
**2. Evaluation approach**

The evaluated data are based mainly on the modern theoretical model calculations with MCFx code system [1-20]. The developed code system is destined to the detailed description of all stages of nucleon-induced reactions on heavy nuclei for  $E > 20$  MeV including:

- description of entrance channel in the framework of optical model and coupled channel method (OM);
- simulation of direct processes with intranuclear cascade model (INC);
- simulation of pre-equilibrium multi-particle emission (MCP);
- description of fission/evaporation competitions on the base of Hauser-Feshbach statistical model (SM);
- description of primary fission fragment formation and yields with new potential model of octupole nuclear shape oscillations (PFF);
- calculation of secondary fission fragment yields after particle evaporation (SFF).

The block scheme of the calculation flow is presented in the Fig.1.1

**Fig.1.1 Block scheme of the MCFx code and calculation flow**



Here  $n$  ( $p$ ) is the incident neutron (proton),  $A$ ,  $Z$ -mass and charge of the target nuclei. At the first stage the reaction cross section is calculated which serves as a normalization factor for the calculation of absolute cross sections. Then, after the emission of fast particles in the cascade stage, the distribution of the residual nucleus  $Y$  ( $A_i, Z_i, E^*$ ;  $ph$ ) with different mass and charge numbers ( $A_i, Z_i$ ), excitation energies ( $E_i^*$ ) and the number of excitons ( $ph$ ) is formed which decay to equilibrium state ( $A_j, Z_j, E_j^*$ ) by pre-equilibrium emission of particles.

## 2.1 Entrance channel.

Extension of a beam energy range up to a few GeV needed some modification of the previously developed KRI2000 optical model parameterization [3]. Namely, potentials have been simplified slightly; energy dependence has been included in the spin-orbit part; the unphysical linear functions (which are convenient in a narrow energy range) have been replaced by the exponential dependences; some additional fit has been carried out to describe the experimental data available for the projectile energy up to 1 GeV. The new optical model parameter set was created by a fitting to experimental cross sections for wide target mass region. The optical model itself guarantees good description of the nucleon elastic scattering. Indeed, the changing of the differential cross sections is 8-10 orders of magnitude. The calculated data differ from the measured ones for the negligible values only.

Parameterization of new optical model potential has the following form:

Neutrons:

$$\begin{aligned}
 V_r(E) &= (48.65 - 15.22\eta)(1 - 0.0052E), & 10 < E \leq 100 \text{ MeV}, \\
 &= (62.78 - 16.16\eta) \exp(-E/100), & 100 < E \leq 1000 \text{ MeV}, \\
 r_r &= 1.26, \quad a_r = 0.626; \\
 \\
 W_v(E) &= 1 + \frac{10.0}{1 + \exp[(51.0 - E)/10]} - 4\eta, & 10 < E \leq 80 \text{ MeV}, \\
 &= 15.658 + 6.5 \ln(E/180) - 4\eta, & 80 < E \leq 1000 \text{ MeV}, \\
 r_{wv} &= 1.20, \quad a_{wv} = 0.666; \\
 \\
 W_d(E) &= (8.88 - 6.06\eta) \left\{ 1 - \frac{1}{1 + \exp[(40.0 - E)/15]} \right\}, & E \geq 10 \text{ MeV}, \\
 \\
 r_{wd} &= 1.26, \quad a_{wd} = 0.535;
 \end{aligned} \tag{2.1}$$

Protons:

$$\begin{aligned}
V_r(E) &= (48.65 + 15.22\eta)(1 - 0.0052E), & 10 < E \leq 100 \text{ MeV}, \\
&= (62.78 + 16.16\eta) \exp(-E/100), & 100 < E \leq 1000 \text{ MeV}, \\
r_r &= 1.26, \quad a_r = 0.626; \\
\\
W_v(E) &= 1 + \frac{10.0}{1 + \exp[(51.0 - E)/10]} + 4\eta, & 10 < E \leq 80 \text{ MeV}, \\
&= 14.96 + 6.5 \ln(E/180) + 4\eta, & 80 < E \leq 1000 \text{ MeV}, \\
r_{wv} &= 1.20, \quad a_{wv} = 0.72; \\
\\
W_d(E) &= (8.88 + 6.06\eta) \left\{ 1 - \frac{1}{1 + \exp[(40.0 - E)/15]} \right\}, & E \geq 10 \text{ MeV}, \\
\\
r_{wd} &= 1.26, \quad a_{wd} = 0.72;
\end{aligned} \tag{2.2}$$

$$V_{so}(E) = 10.72 \exp(-E/160), \quad r_{so} = 1.20, \quad a_{so} = 0.500.$$

## 2.2 Intranuclear cascade.

Dubna version of intranuclear cascade model was used. The main parameter in the intranuclear cascade model is so-called cut-off energy  $E_{cut}$  that is minimal energy of fast particle inside the nuclear volume where the further development of the intranuclear cascade is impossible. Choice of this parameter strongly depends from used calculation scheme and parameters of other models and as a rule  $E_{cut}$  is equal to 10-20 MeV. In such a case emitted nucleons cannot have energy less than  $E_{cut}$  and calculated spectrum will be discontinuous. The spectrum of this form cannot be explained by physical considerations or by experimental facts. We replaced the cut off threshold by the parabolic barrier with fixed height  $B \sim 10$  MeV and width  $W \sim 50$  MeV. So it is smooth slowing down of an INC contribution to the reaction cross sections as a projectile energy decreases [15].

## 2.3 Preequilibrium multiparticle emission.

In the proposed scheme of preequilibrium calculation (model MCP) [9,10] the reaction begins with various initial excitations and configurations, residual nucleus should pass to equilibrium emitting out the nucleons. One problem exists in this situation: in what time moment can one believe the system is at equilibrium? The physical criteria of the equilibration time



choice is proposed [20]. The comparison of calculated neutron multiplicities in  $^{208}\text{Pb} + p$  reaction with experimental data has served as the basis for the testing of the proposed method. It is appeared, that calculated neutron multiplicities are in good coincidence with experimental data without parameter fitting.

## **2.4 Fission fragment formation**

The new potential model [14] for fission yields calculations were developed. The fission fragment formation is considered as the neck instability in the process of octupole oscillations of neutrons and protons near the scission point. To describe such a phenomenon the potential surface of fissioning nucleus with neck radius about 1 fm was calculated with shell correction approach. The new version of smooth liquid drop part of the deformation energy is proposed. The liquid drop part is formulated in a double folding model with n-n, p-p, and n-p Yukawa' interaction potential. Fission fragment mass and charge distributions correspond to isoscalar and isovector modes of vibrations and are defined by wave functions of oscillations.

## **3. Comparison with experimental data and other evaluations and compilation of results**

### **3.1 Comparison with experimental data and other evaluations**

#### **3.1.1 Fission cross-sections**

Our results on fission cross-sections evaluations are compared below with available experimental data and JENDL/HE-2007 evaluations (except  $^{232}\text{Th}$  where no data found in the JENDL/HE-2007 library). Experimental data were taken from compilations [21,22] as well as from work [23] and EXFOR database (original works are [24-32]).

#### **$^{202}\text{Hg}(n,f)$ и $^{202}\text{Hg}(p,f)$ .**

The measured cross sections are not available for this target. The calculations of the fission cross sections were done after the description of the experimental data on fission of the  $^{208}\text{Pb}$  and  $^{209}\text{Bi}$  targets by the neutrons and protons. The contributions to total fission cross sections of  $^{202}\text{Hg}(n,f)$  and  $^{202}\text{Hg}(p,f)$  reactions are from the fissile nuclei which take place in the fission of the  $^{208}\text{Pb}$  and  $^{209}\text{Bi}$  targets at the high projectile energies. The usage of the barriers approved at the experimental data descriptions leads to the increasing of the cross section predictability (Fig.3.1). It is obvious that in this case the differences between the neutron fission and the proton

fission cross sections are small for all beam energies. The cross section increasing for near-barrier fission at low nucleon energies (20-40 MeV) is the result of the fission probability increasing, but not the result of coulomb barrier penetrability increasing. The values of fission barrier are 30-25 MeV, the proton coulomb barrier are 8-10 MeV for this target masses.

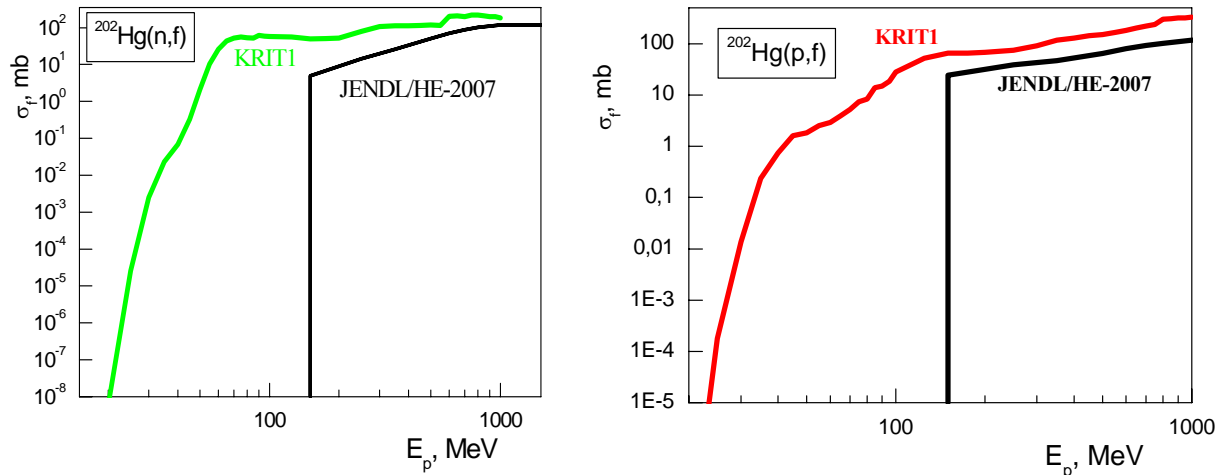


Fig. 3.1. Fission cross section of  $^{202}\text{Hg}$  by neutrons and protons. Curves are the KRITI library evaluated data and JENDL/HE-2007 data.

**$^{208}\text{Pb}(n,f)$** . The experimental data are available up to 200 MeV neutron energy (Fig.3.2). All measurements have been done in Gatchina at different time. The modern data by Laptev e.a. were described by MCFx method without parameter fitting practically for the energies higher then 60 MeV. Some structure at 30-40 MeV (Fig. 3.2) of the experimental data exists, but it was not our aim to fit these data. These data are of course very interesting form the theoretical point of view, but they are negligible as practical data because of very small values. The calculated curve of fission cross section becomes the constant value 50-60 mbarns for the energies more than 200 MeV.

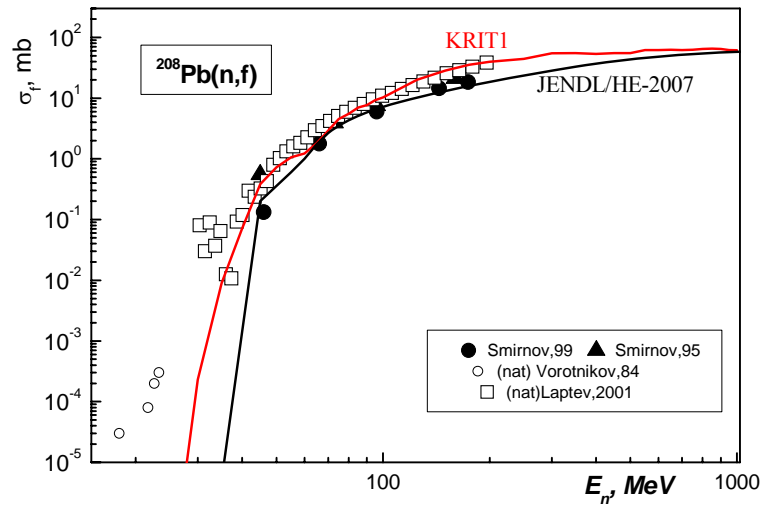


Fig. 3.2. Fission cross section of  $^{208}\text{Pb}$  by neutrons. Curves are the KRIT1 library evaluated data and JENDL/HE-2007 data, symbols show experimental results.

**$^{208}\text{Pb}(p,f)$ .** This cross section was good investigated experimentally for the proton energy region from 200 MeV to 1000 MeV (Fig.3.3). The data by all groups are in reasonable coincidence with the exception of the old data by Bochagov e.a measured in 1978 for 1000 MeV. The data by Bochagov e.a. seem to be wrong. The results of our calculations are fitted to the Kotov e.a. data and they describe the measured data inside the experimental data corridor.

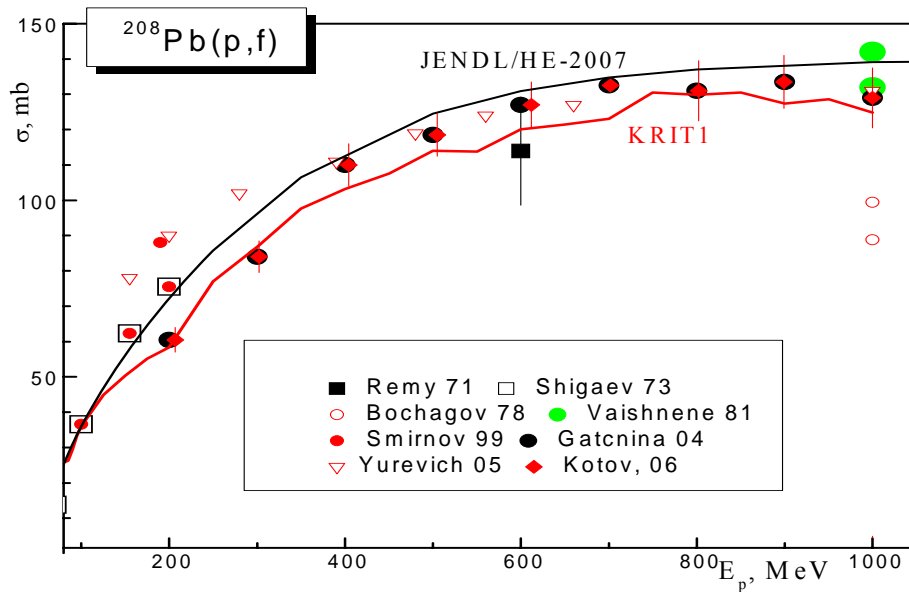


Fig. 3.3. Fission cross section of  $^{208}\text{Pb}$  by protons. Curves are the KRIT1 library evaluated data and JENDL/HE-2007 data, symbols show experimental results.

**$^{209}\text{Bi}(n,f)$** . The modern experimental data are available for the beam energies up to 200 MeV (Fig.3.4). Besides of these data, the old (1955 y.) measured cross sections by Goldanskiy e.a. exist. The theoretical curve coincides with the measured values for the energies greater then 60 MeV. We used eye guide evaluation based on the data by Vorotnikov e.a. and Laptev e.a. to get the results for KRIT1 library.

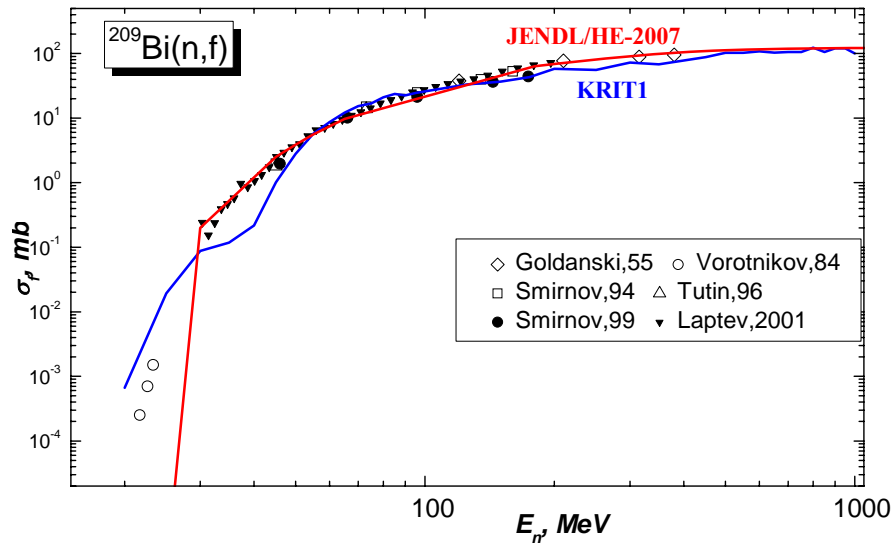


Fig. 3.4. Fission cross section of  $^{209}\text{Bi}$  by neutrons. Curves are the KRIT1 library evaluated data and JENDL/HE-2007 data, symbols show experimental results.

**$^{209}\text{Bi}(p,f)$** . The modern experimental cross sections are available for the proton energies from 20 MeV up to 1 GeV. These data are reproduced by the calculations reasonably good (Fig.3.5).

**$^{232}\text{Th}(n,f)$** . The results by Lisowski e.a. up to 250 MeV and the modern measurements by Laptev e.a. up to 200 MeV are available for this reaction. The data of both groups coincide in the frame of experimental errors. The theoretical results describe these data in the region of 20-100 MeV (Fig.3.6). The calculated curve is in good coincidence with the Lisowski's data for the energies greater than 100 MeV. It should be point out that there is the surprise behavior of the energy dependence of the calculated fission cross section: the cross section increasing from 750 to 1000 mbarns at the energies 250-1000 MeV instead of the constant cross section value.

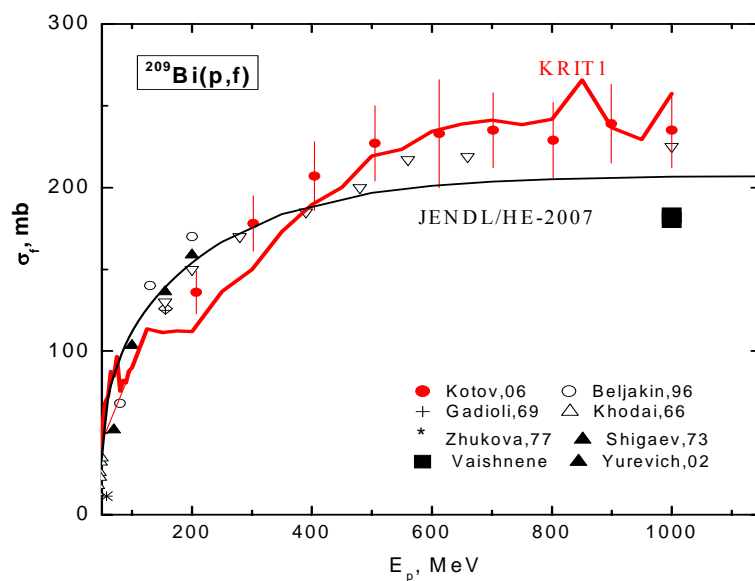


Fig. 3.5. Fission cross section of  $^{209}\text{Bi}$  by protons. Curves are the KRIT1 library evaluated data and JENDL/HE-2007 data, symbols show experimental results.

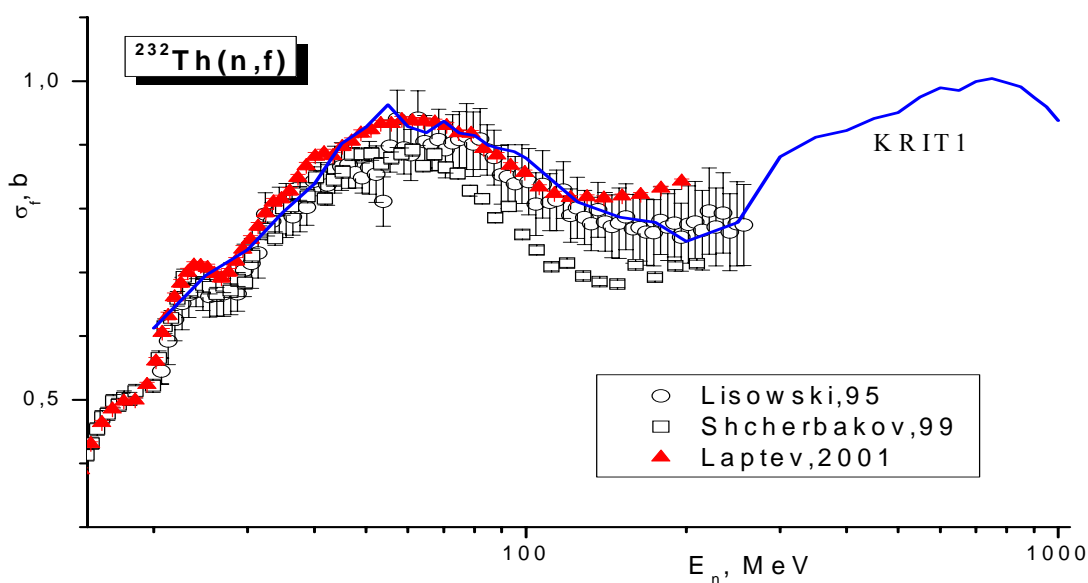


Fig.3.6. Fission cross section of  $^{232}\text{Th}$  by neutrons . The symbols are the experimental data, the curve is the KRIT1 library evaluation – the results of MCFx calculations.

**$^{232}\text{Th}(p,f)$ .** The general view of the fission cross section of  $^{209}\text{Bi}$  by protons is presented in Fig.3.7. The reaction was the subject of a long time investigations. The modern data by Eismont e.a. (20-80 MeV), the new data by Kotov E.a. (200-1000 MeV) and the measurements by

Shigaev e.a were the base of our evaluation which is the results of the theoretical calculations with MCFx code. We did not take into consideration the old measurement results: 600-700 mbarns at 300-700 MeV, and the single points at 1000 MeV. A lot of data at the energies smaller than 20 MeV do not coincide with the data we used for evaluation.

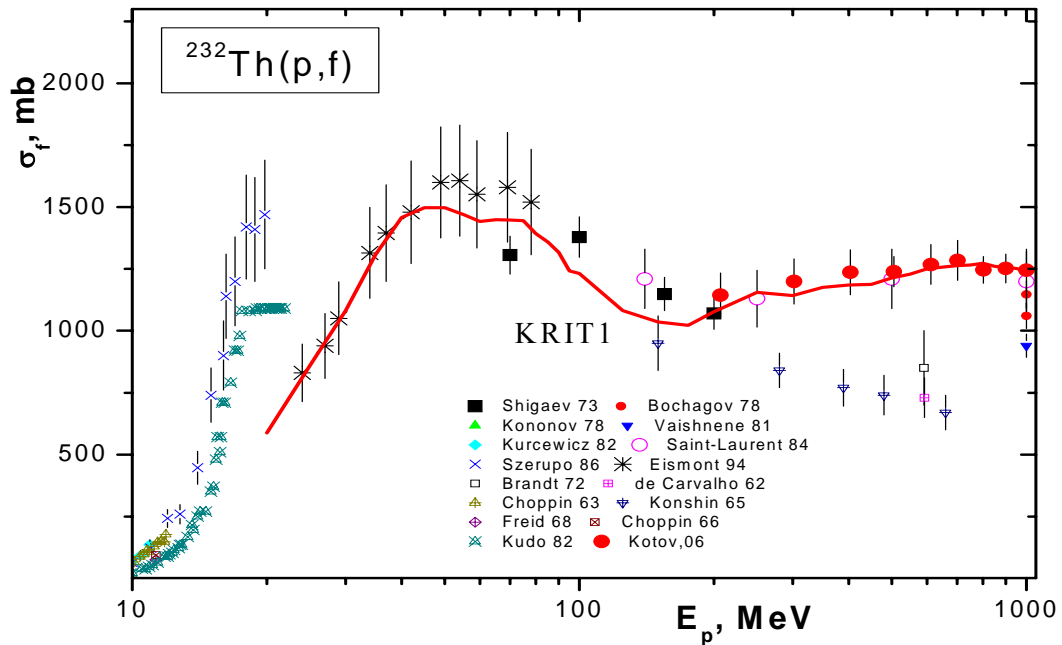


Fig.3.7. Fission cross sections of  $^{232}\text{Th}$  by protons . The symbols are the experimental data, the curve is the KRIT1 library evaluation – the results of MCFx calculations.

$^{235}\text{U}(n,f)$ . The evaluation is based on the results of calculations fitted to the single experimental data set by Lisowski e.a. (1995 y.) The measured data description (Fig.3.8) was done by the fission barriers changing.

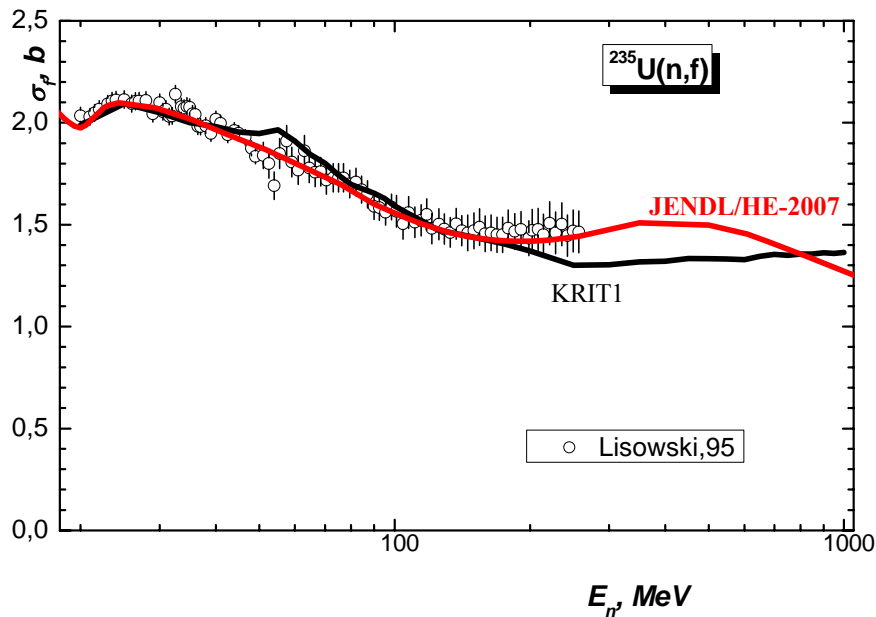


Fig. 3.8. Fission cross section of  $^{235}\text{U}$  by neutrons. Curves are the KRIT1 library evaluated data and JENDL/HE-2007 data, symbols show experimental results.

**$^{235}\text{U}(p,f)$ .** The measured data by the six groups are available. The modern (1994 y.) data by Eismont e.a. (20-80 MeV), The new (2005 y.) data by Kotov e.a. (200-1000 MeV) and the measurements by Bychenkov e.a. (80-200 MeV) were described by the theoretical results reasonably good (Fig.3.9).

**$^{238}\text{U}(n,f)$ .** The measured cross sections by Laptev e.a (2001 y.) are smaller than the data by Lisowski e.a (1995 y.) by 10-15 percents for all energy region from 20 to 200 MeV. The theoretical results are very sensitive on the model parameters in this energy range. So, we could get the average cross section values only with the detailed balance of the barrier heights to extrapolate reasonably the theoretical calculations for the high energies where the experimental data are absent. The KRIT1 evaluation for 20 – 200 MeV was done by eye guide method. The KRIT1 evaluation for 200 – 1000 MeV is the results of the theoretical calculations with the parameters fixed in previous energy region (Fig.3.10).

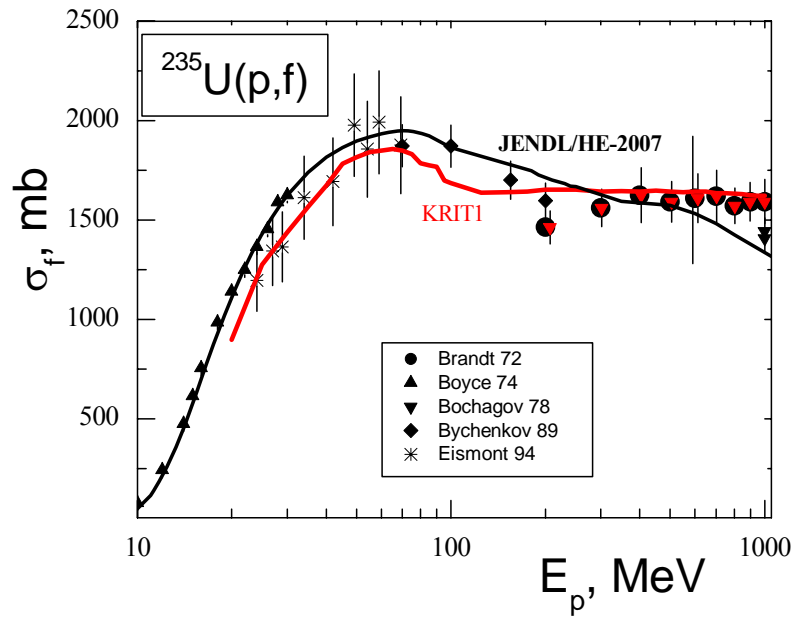


Fig. 3.9. Fission cross section of  $^{235}\text{U}$  by protons. Curves are the KRIT1 library evaluated data and JENDL/HE-2007 data, symbols show experimental results.

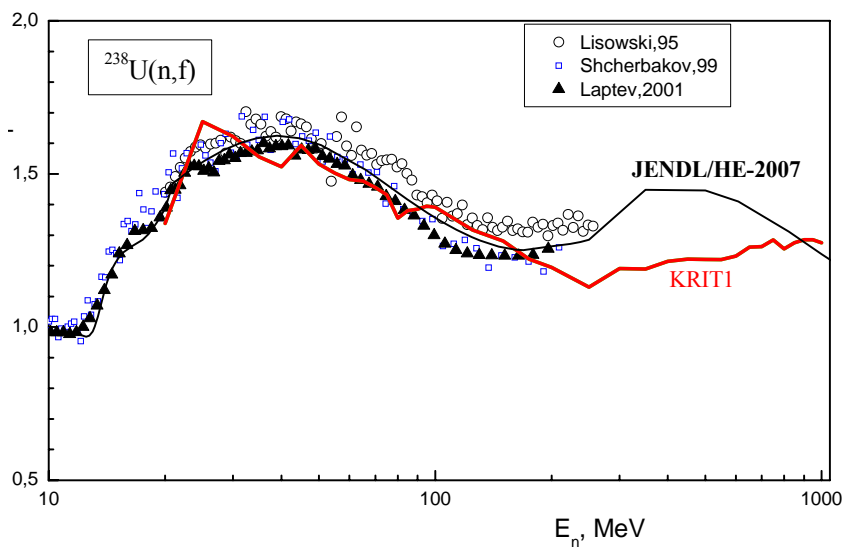


Fig. 3.10. Fission cross section of  $^{238}\text{U}$  by neutrons. Curves are the KRIT1 library evaluated data and JENDL/HE-2007 data, symbols show experimental results.

**$^{238}\text{U}(p,f)$ .** This reaction cross section was investigated experimentally during more than 50 years by more than 30 groups (fig.3.11). We used the modern (1994 y.) data by Eismont e.a. (20-80 MeV), the new data by Kotov e.a. (2006 y.), the data by Baba e.a. (20-60 MeV), the data by



Bychenkov e.a. (80-200 MeV) as the experimental base of evaluation. The theoretical results describe the experimental data base with the small barrier changing.

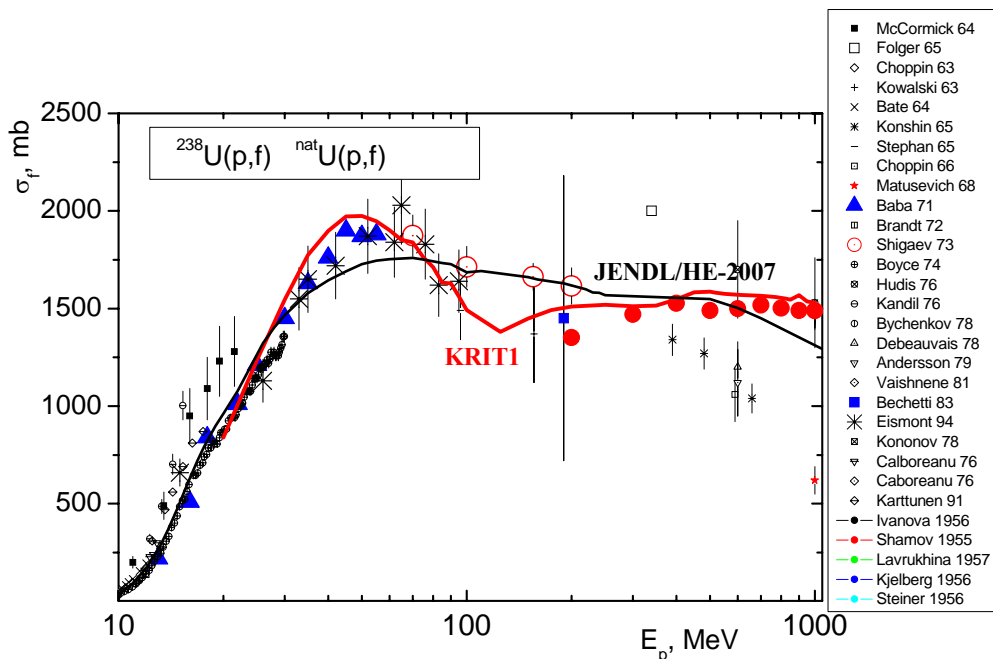


Fig. 3.11. Fission cross section of  $^{238}\text{U}$  by protons. Curves are the KRIT1 library evaluated data and JENDL/HE-2007 data, symbols show experimental results.

So, comparison of our evaluations with JENDL/HE-2007 displays more or less similar results with the exception of mercury case where in the JENDL/HE-2007 fission barrier is obviously strongly overestimated.

### 3.1.2 Independent yields of fission fragments

Data on the yields of fission fragments for out of the reactor energies are practically absent. Only recently researchers from Russia, Sweden, Finland and the U. S. have began data accumulation in the intermediate (typically up to 100 MeV) energy range. To date, the EXFOR contains 12 references to the results of systematic measurements of bismuth, thorium, uranium and neptunium proton- and neutron-induced fission.

To test the model of the formation of fission fragments at the breakpoint in the first phase the calculations were done and the results were compared with all the experimental data for the case of thermal fission of uranium and plutonium, they are shown in Fig. 3.12 and 3.13.

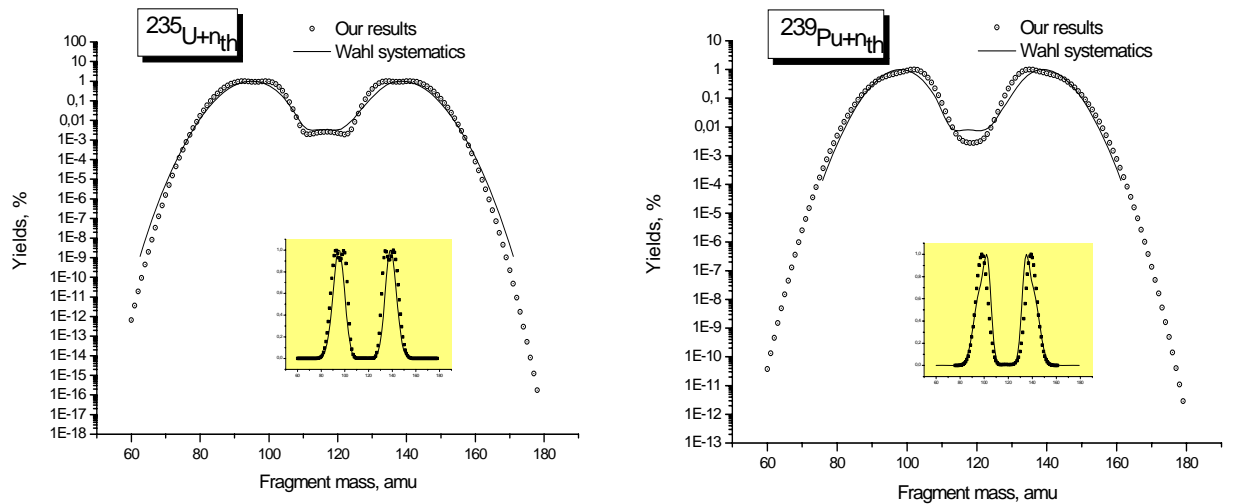


Fig.3.12. Mass distribution of fragments of the thermal fission of uranium and plutonium. The insets show the results in a linear scale.

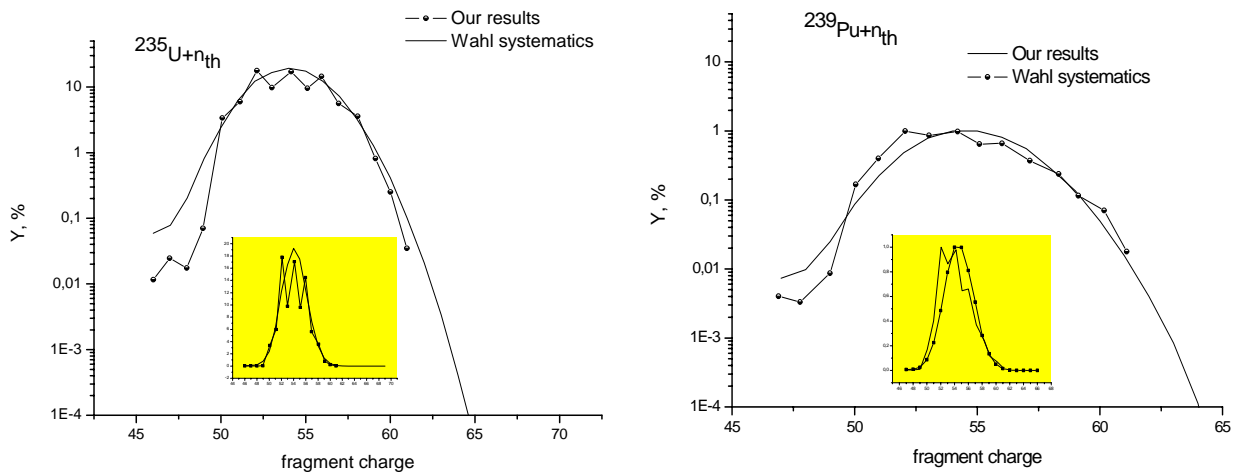


Fig. 3.13. Same as in Fig.3.12, but for the charge distributions of the fragments.

As it can be seen from the figures, the results of calculations reproduce the basic integral data on mass and charge distributions of the fragments well. At the same time, the calculations do not reproduce the structural effects observed in the average values and widths isobaric charge distributions (Fig. 3.14), although they reproduce them on average. The average value of the charge in the isobaric chain is shown in Fig. 3.14a in standard form of deviation of the charge

taken in the assumption of constant charge density  $Z_{UCD} = \frac{Z}{A} A_f$ ,  $Z, A, A_f$  - charge and mass numbers of the fissioning nucleus and the nucleus-fragment, respectively.

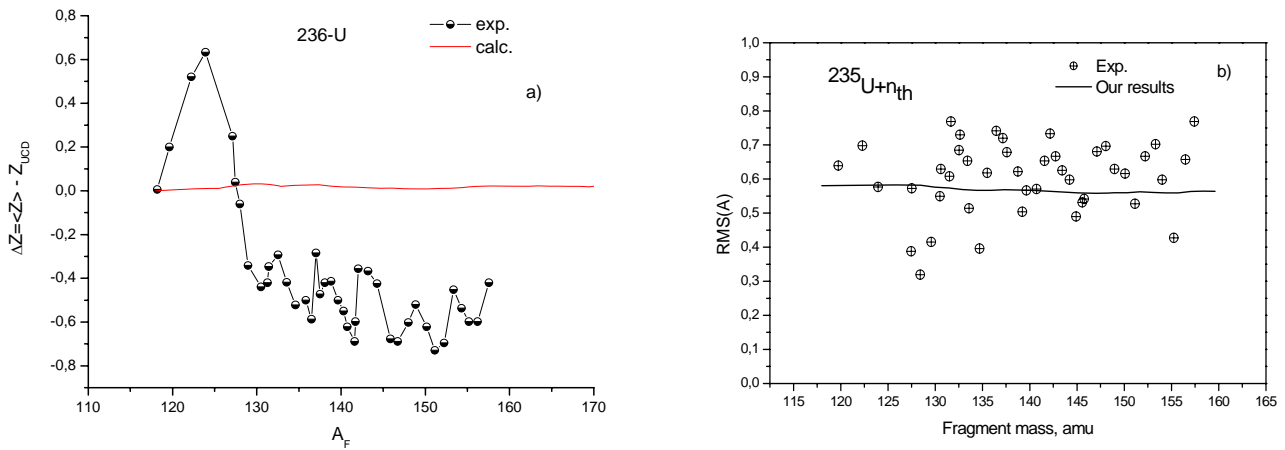


Fig. 3.14. Mean value (a) and rms widths (b) of isobaric charge distributions.

As beam energy increases it is necessary to consider the contributions from the various fissioning nuclei. Then the full distributions will have the form  $Y(A_f) = c \sum \sigma_i Y_i(A_f)$ , where  $\sigma_i$  - the contribution to the total fission cross section of the  $i$ -th fissile nucleus, calculated using the developed MCFx code,  $c$  - normalization constant determined by the condition

$$\sum_{\text{all fragments}} Y(A_f) = 200\%.$$

Examples of the calculation of such partial cross sections for the fission of thorium and uranium are shown in Fig. 3.15 (see also [34]).

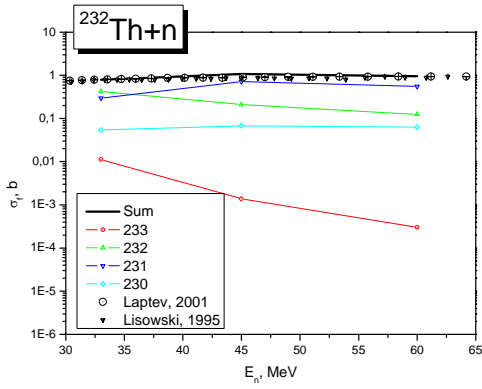


Fig. 3.15a. Total and partial fission cross sections  $^{232}\text{Th}$ .

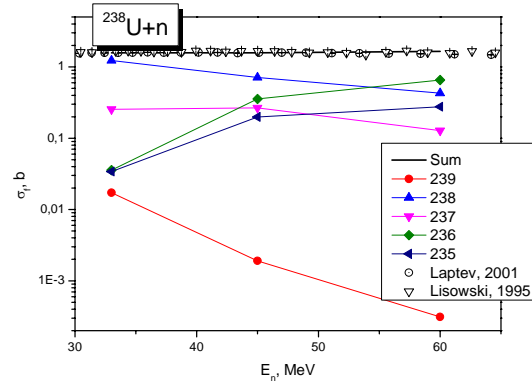
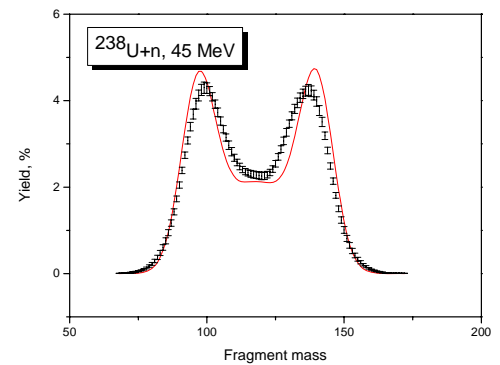
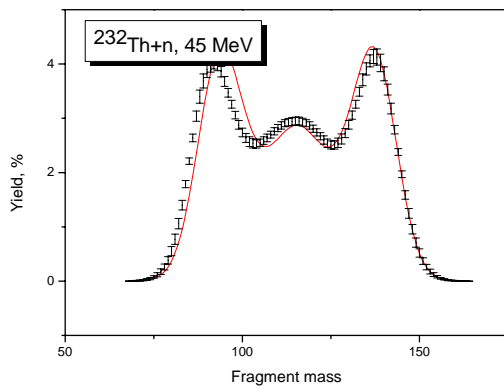
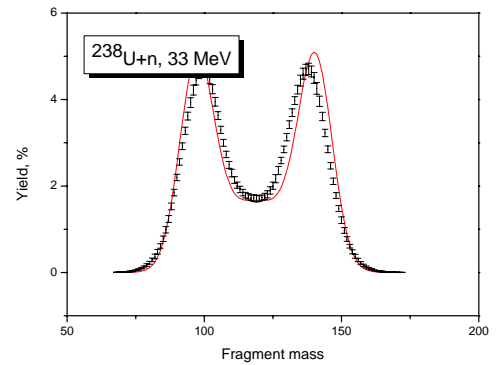
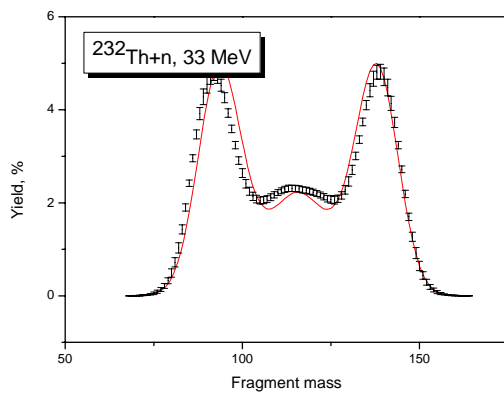


Fig. 3.15b. Total and partial fission cross sections  $^{238}\text{U}$ .

The results of calculations of the mass distributions for these two cases are shown in Fig. 3.16. As can be seen, a model reproduces the experimental data [34] well.



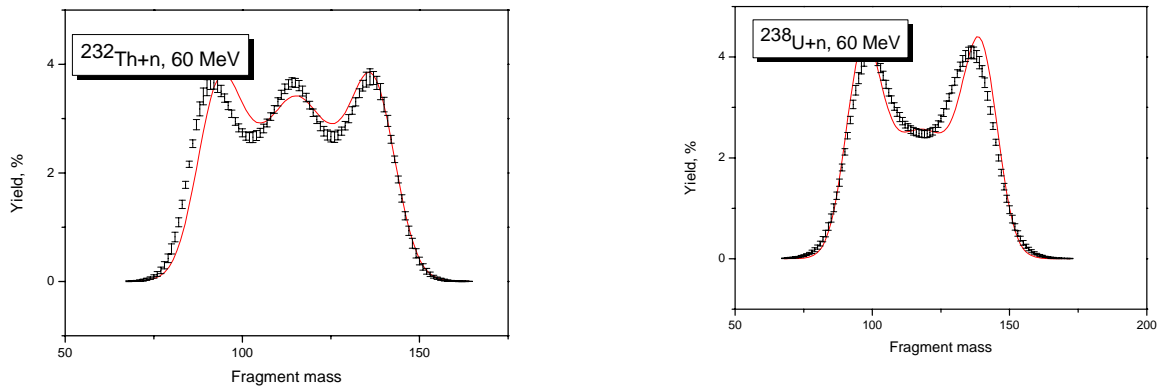
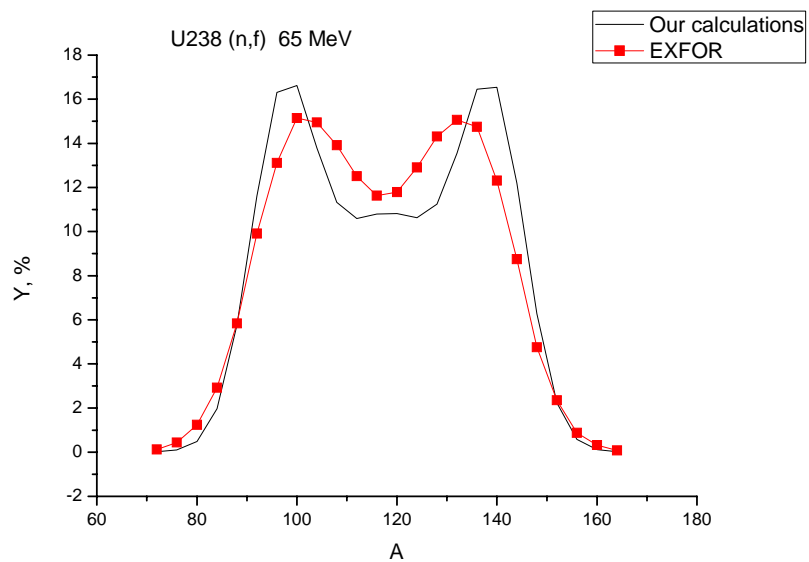
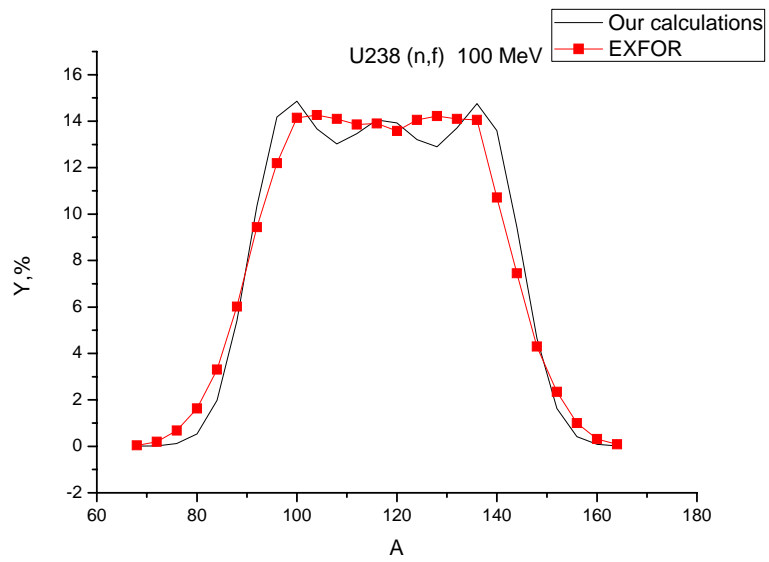
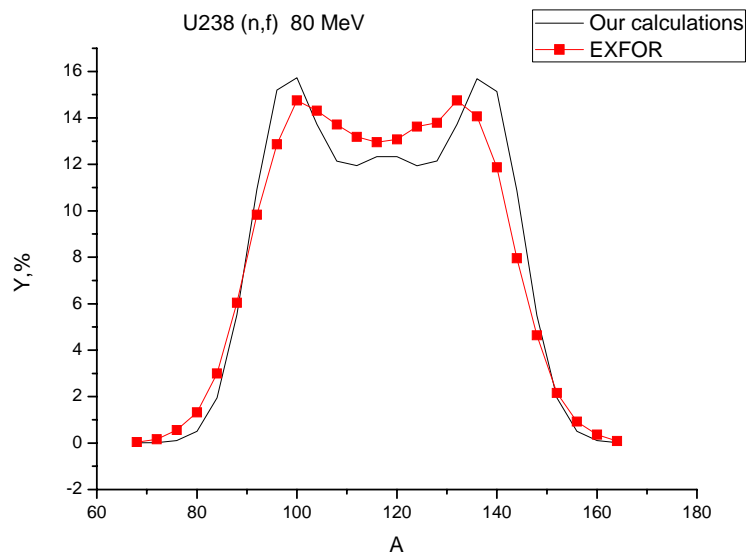
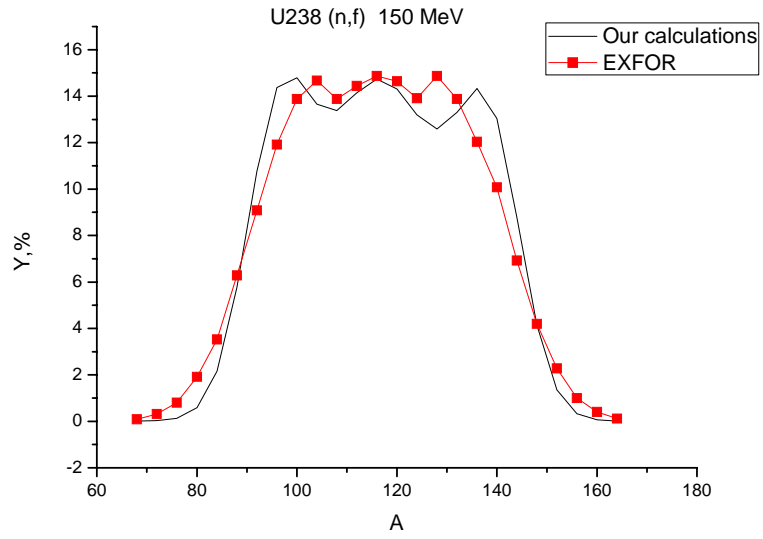
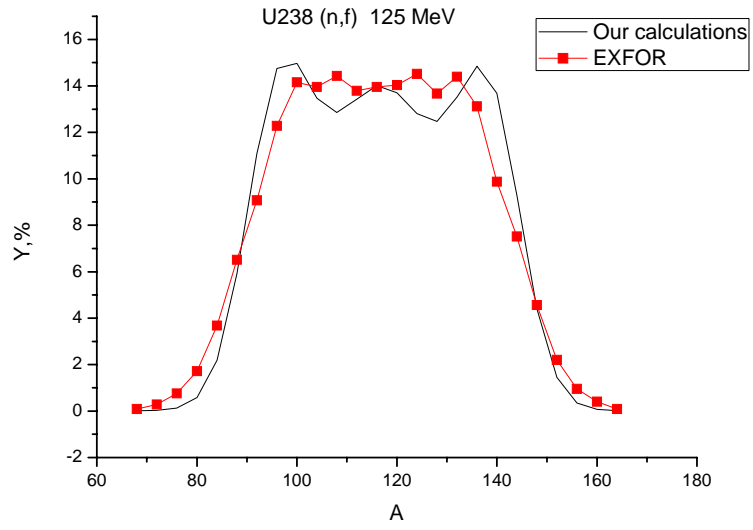


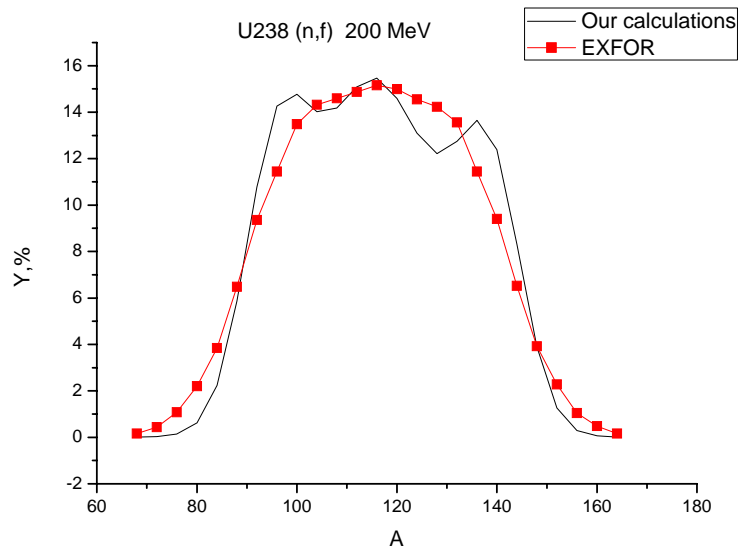
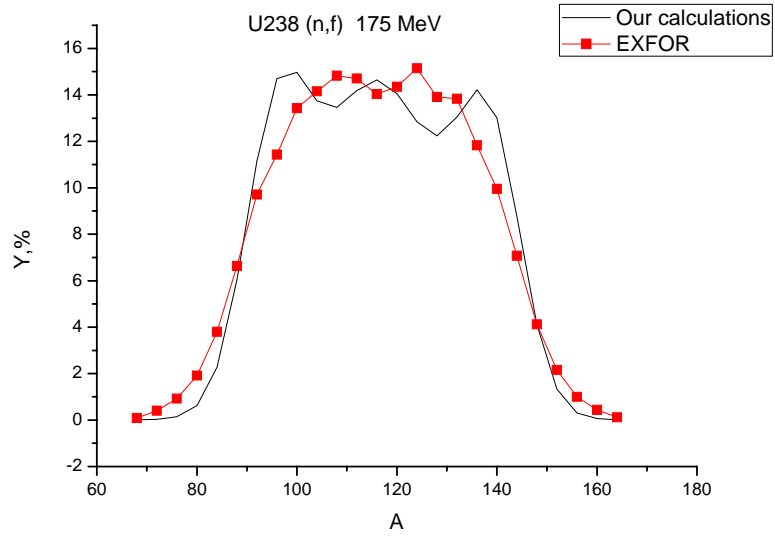
Fig. 3.16. Mass distribution of fission fragments for the  $^{232}\text{Th}+n$  and  $^{238}\text{U}+n$  reactions at neutron energies 33, 45 and 60 MeV.

The following figures shows the comparisons of our calculations of the mass distributions with all experimental data presented in the EXFOR library and corrected by the authors of these works for the emission of neutrons. All calculations were made in a uniform approach without variation of parameters.

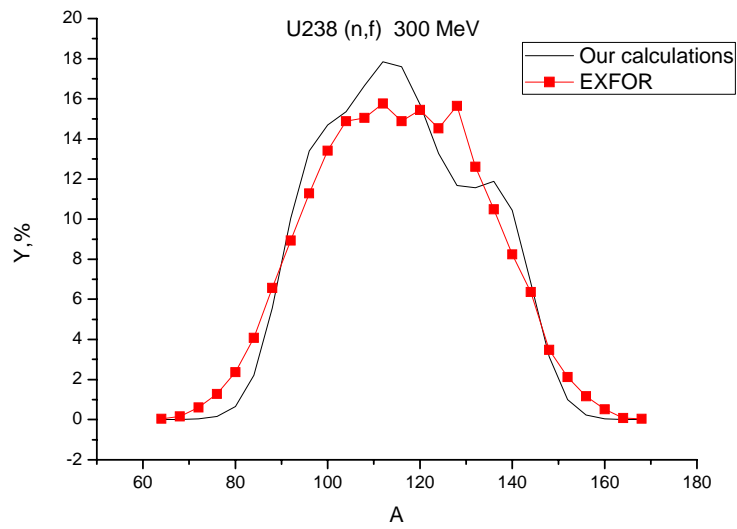
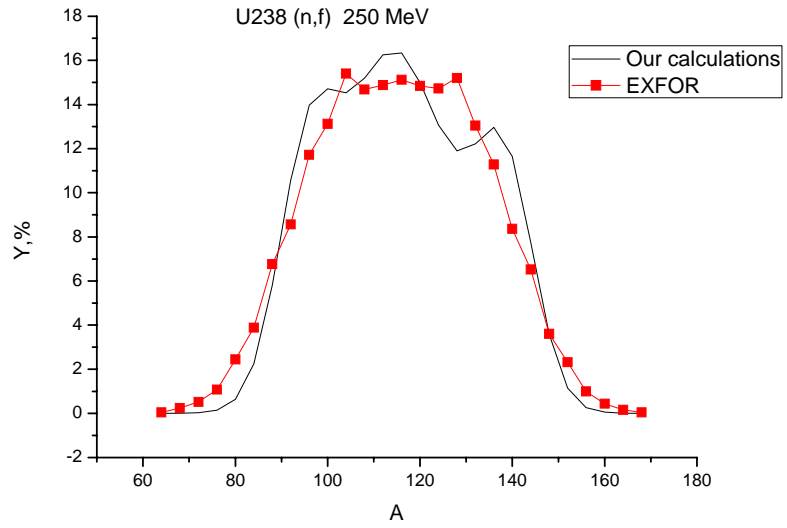












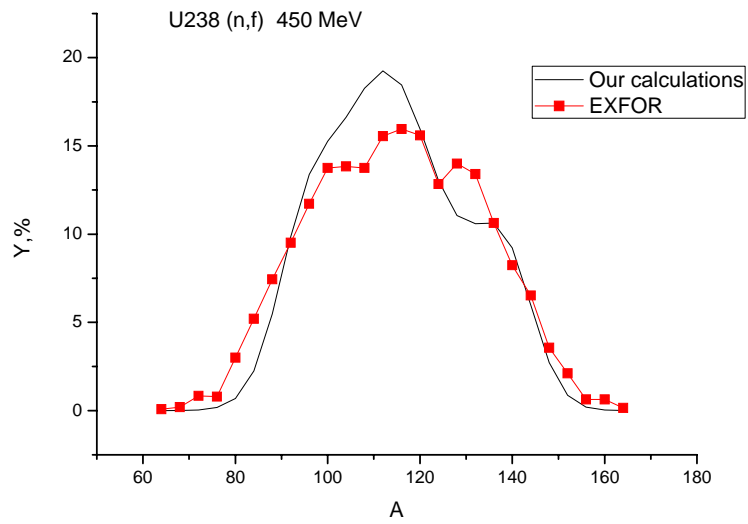
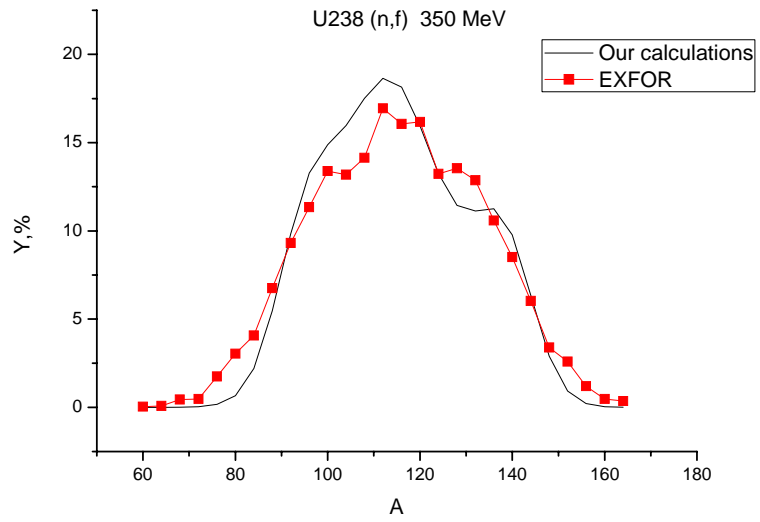


Fig. 3.17. Mass distribution of fission fragments in the  $^{238}\text{U} + n$  reaction.

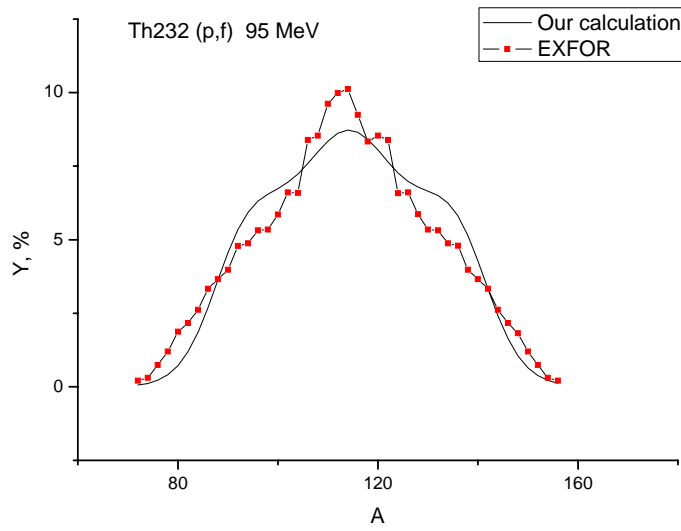
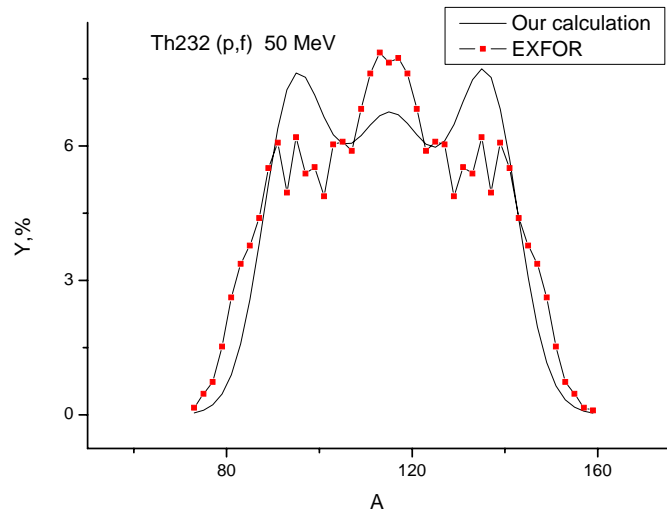
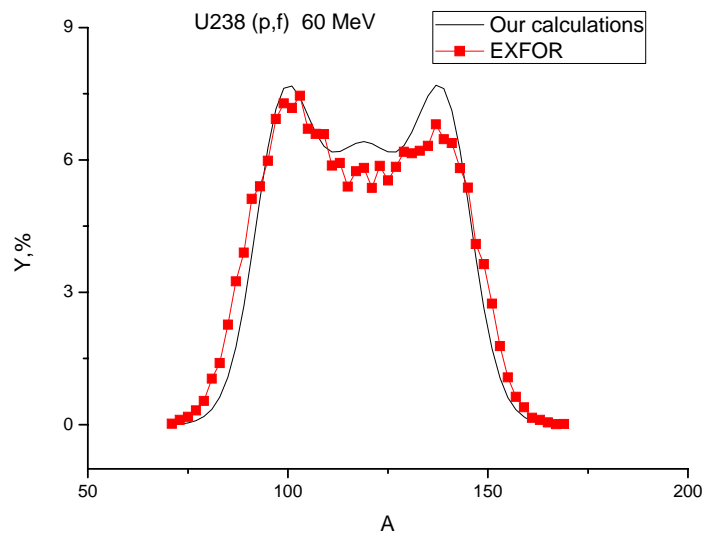
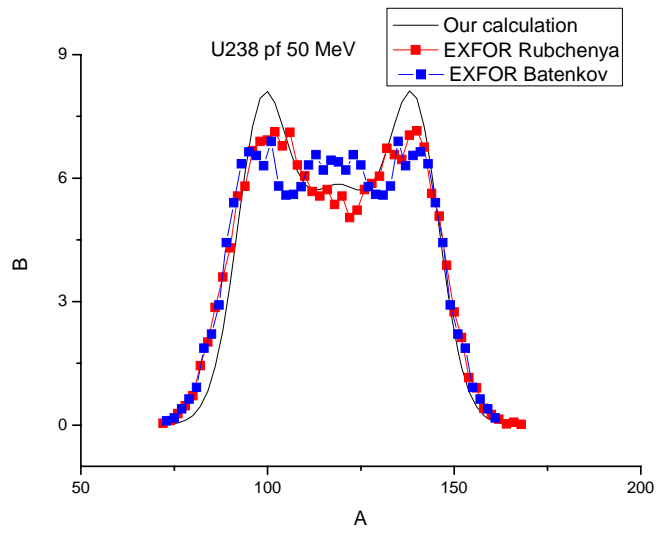
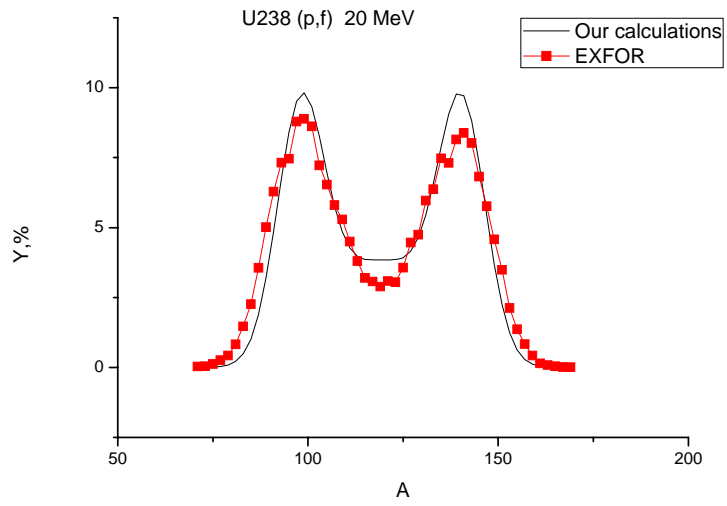


Fig. 3.18. Mass distribution of fission fragments in the  $^{232}\text{Th} + \text{p}$  reaction.



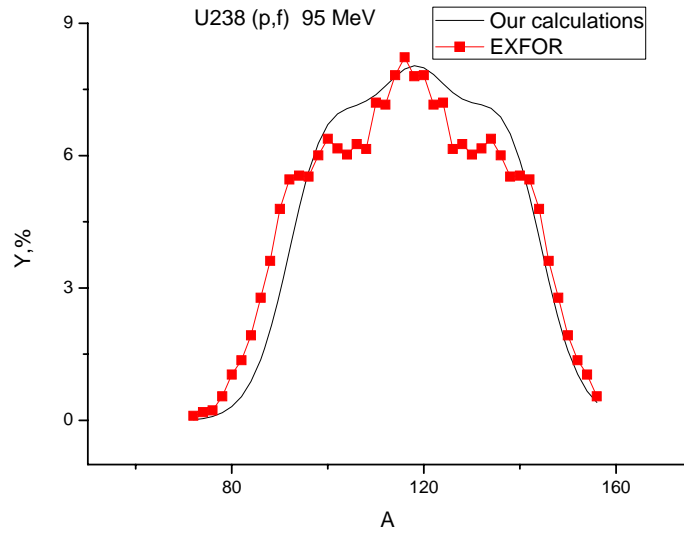
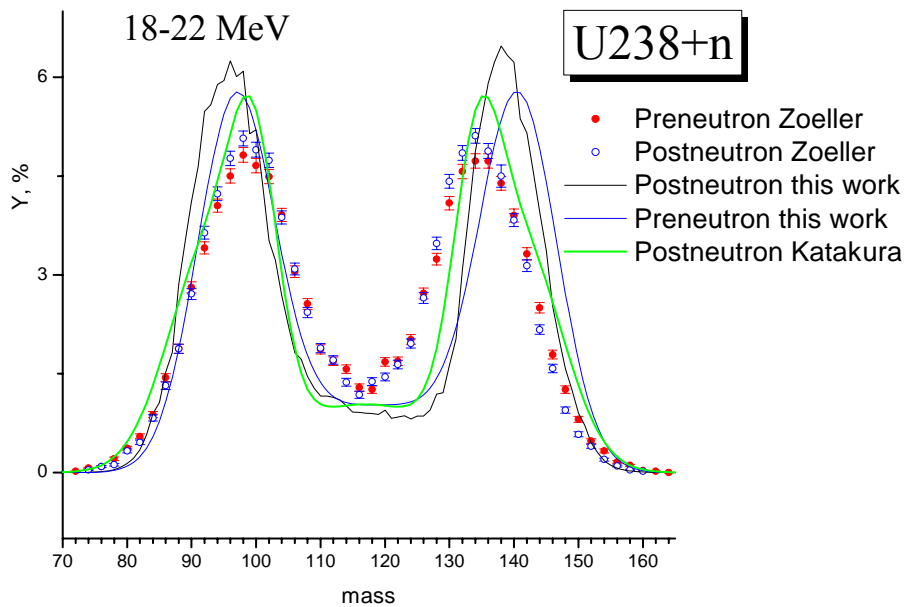
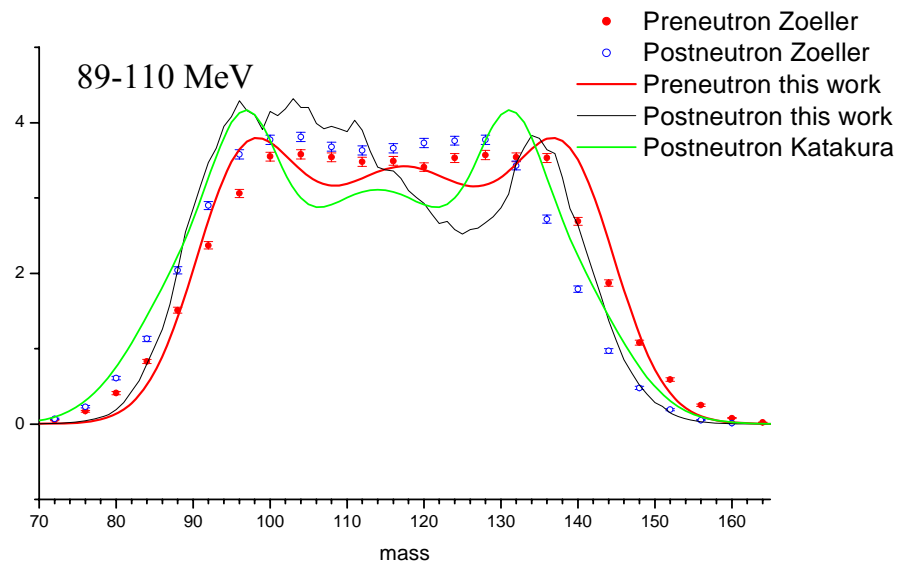
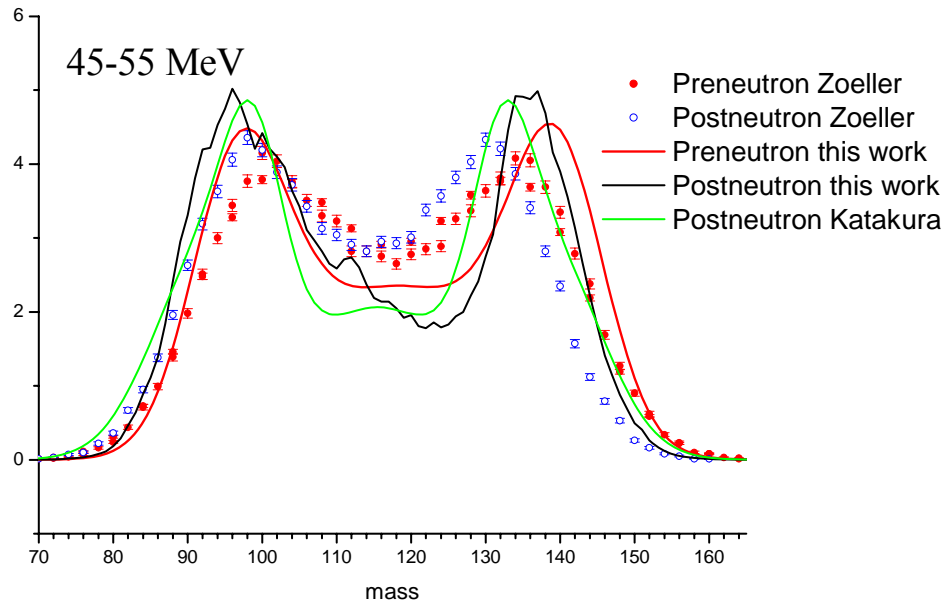


Fig. 3.19. Mass distribution of fission fragments in the  $^{238}\text{U} + \text{p}$  reaction.

To correct our data for neutron emission from excited fission fragments the special statistical Hauser-Feshbach calculations have been done for about 1500 fragment nuclei excited up to 150-200 MeV. Comparison of our results with experimental data for cold (postneutron) fission fragment mass distribution and systematics of Katakura [35] is presented in the Fig. 3.20.





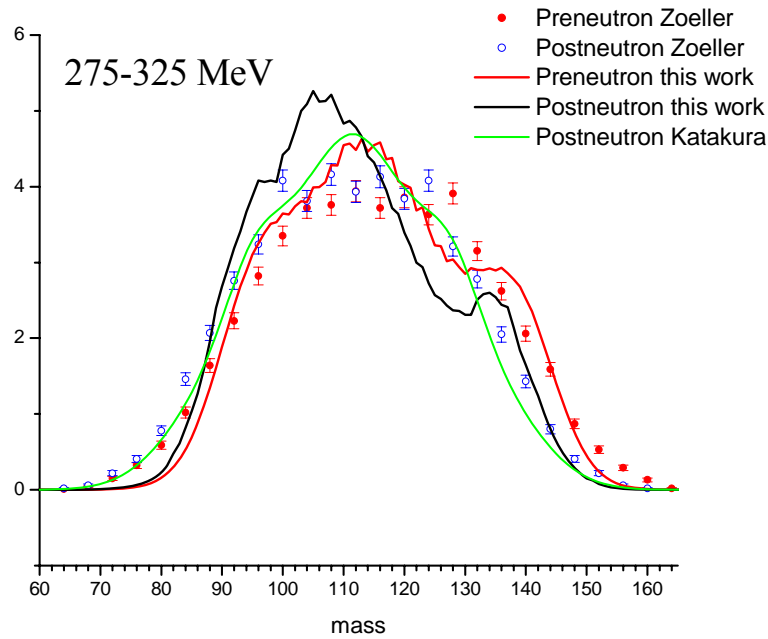


Fig. 3.20. Fission fragment mass distribution: red symbols are preneutron experimental data, blue ones are postneutron experimental data, red and black lines are our results for preneutron and postneutron cases, correspondingly. Green line corresponds to [35].

### 3.2 Data compilation

Results of calculations were tabulated in four transport and fission yields ENDF-6-formatted libraries – **KRIT1n**, **KRIT1p** (Khlopin Radium Institute Transport neutron/proton) for cross-sections and energy-angle distributions of emitted particles and **KRIFFn**, **KRIFFp** (Khlopin Radium Institute Fission Fragments neutron/proton) for independent and cumulative fission yields. Each library includes 12 files for neutron- or proton-induced fission of  $^{202}\text{Hg}$ ,  $^{208}\text{Pb}$ ,  $^{209}\text{Bi}$ ,  $^{232}\text{Th}$ ,  $^{235}\text{U}$ ,  $^{238}\text{U}$  within nucleon energy region 20-1000 MeV.

#### 3.2.1 Contents of KRIT1 Library

**MF=1** GENERAL INFORMATION

MT=452 NUMBER OF NEUTRONS PER FISSION (MCFx CALCULATIONS)

**MF=2** RESONANCE PARAMETERS

MT=151 RESONANCE PARAMETERS (Potential Scattering Radius only)

**MF=3 REACTION CROSS SECTIONS**

MT=1 TOTAL CROSS SECTION (ECIS CALCULATIONS)

MT=2 ELASTIC SCATTERING (ECIS CALCULATIONS)

MT=5 TOTAL-ELASTIC-FISSION=NUCLEON PRODUCTION XS (MCFx CALCULATIONS)

MT=18 TOTAL FISSION (HAUSER-FESHBACH CALCULATIONS BASED ON FISSION BARRIERS)

**MF=4 ANGULAR DISTRIBUTION OF SECONDARY**

MT=18 FISSION REACTION (Isotropic Neutrons from Fission Fragments)

**MF=5 ENERGY DISTRIBUTIONS OF SECONDARY NEUTRONS**

MT=18 PROMPT NEUTRONS FROM FISSION (Neutron spectra of Fission Fragments)

**MF=6 PRODUCT ENERGY-ANGLE DISTRIBUTION**

MT=2 ELASTIC SCATTERING (Distribution of elastic scattering - ECIS calculations with KRI2004 OMP set)

MT=5 Neutron and Proton (Neutron and proton distribution)

### 3.2.2 Contents of KRIFF Library

**MF=8 RADIOACTIVE DECAY AND FISSION PRODUCT YIELD DATA**

MT=454 FISSION PRODUCT INDEPENDENT YIELD DATA (Fission Fragment Independent Yields)

MT=459 FISSION PRODUCT CUMULATIVE YIELD DATA (Fission Fragment Cumulative Yields calculated on the base of MT=454 with ENDF/B-VII decay data)

### References.

1. Yavshits S., Boykov G., Ippolitov V., Pakhomov S. VANT, 2000. No. 1. pp.62-71.
2. Yavshits S., Boykov G., Ippolitov V., Pakhomov S. Proc. of the 2000 Symp. On Nuclear Data. 2000. JAERI. Tokai. Japan. Eds. N.Yamano. T.Fukahori. P.277-282
3. Yavshits S., Boykov G., Ippolitov V., Pakhomov S. Proc. of IX International Seminar on Interaction of Neutrons with Nuclei (ISINN-9). 2001.Dubna. P.160-167.



4. Yavshits S., Goverdovskii A., Ippolitov V. Proc. of the International Conference on Nuclear Data for Science and Technologies.. Tsukubo. P.104-107.
5. Yavshits S. Report IAEA-NDS-153. February 2002. <http://www-nds.iaea.org/reports/nds-153.pdf>
6. Yavshits S., Grudzevich O., Ippolitov V., 7th Information Exchange Meeting on Actinide and Fission Product Partitioning and Transmutation. 2002. Jeju. Korea. <http://www.nea.fr/html/pt/docs/iem/nea4454-pt.pdf>
7. Grudzevich O., Yavshits S. Proc. of Int. Conference on Nuclear Data for Science and Technology. 2004. Santa Fe. USA. v.2. P.1221-1225.
8. Yavshits S., Grudzevich O. Proc. of 3rd Int. Workshop on Nuclear Fission and Fission Product Spectroscopy. 2005. Cadarache. France. P.373-275.
9. Grudzevich O.T., Martirosyan J.M., Yavshits S.G. Oxford Journal Radiation Protection Dosimetry. 2007. Neudos-10. Special issue. P.101-103.
10. Martirosyan Yu., Grudzevich O., Yavshits S. Proc. of the XIV International Seminar on Interaction of Neutrons with Nuclei (ISINN-14). Dubna. 2006. P.235-242.
11. Yavshits S., Martirosyan Yu., Grudzevich O. Proc. of the XIV International Seminar on Interaction of Neutrons with Nuclei (ISINN-14). Dubna. 2006. P.75-83.
12. Yavshits S., Grudzevich O. Proc. of Int. Conference on Nuclear Data for Science and Technology. 2007. Nice. France. V.1. P.363.
13. Grudzevich O., Yavshits S. Proc. of Int. Conference on Nuclear Data for Science and Technology. 2007. Nice. France. V.2. P.1213
14. Yavshits S. EPJ Web of Conference 2 (2010) 08004
15. Grudzevich O., Yavshits S. EPJ Web of Conference 2 (2010) 12003.
16. Yavshits S., Grudzevich O. EPJ Web of Conference 2 (2010) 14006.
17. S.Yavshits INDC-CCP-0452 (2011) IAEA. <http://www-nds.iaea.org/reports-new/indc-reports/indc-ccp/indc-ccp-0452.pdf>.
18. I. V. Ryzhov, S. G. Yavshits, G. A. Tutin et al. Phys. Rev. C83 (2011) 054603
19. Yavshits S., Grudzevich O. Journal of the Korean Physical Society 59 (2011) 939.
20. O.T.Grudzevich, S.G. Yavshits. Yadernaya Fizika, 2011, Vol. 74, No. 10, pp. 1411-1419.
21. A. V. Prokofiev, Nucl. Instrum. Methods Phys. Res. A **463**, 557 (2001).
22. A. I. Obukhov, Phys. Part. Nucl. **32**, 162 (2001).
23. A. Kotov, Phys. Rev., **4**, 034605 (2006).
24. J.R.Boyce, T.D.Hayward, R.Bass et al. Phys. Rev. **C10** (1974) 231.
25. B.A.Bochagov, V.S.Bychenkov, V.D.Dmitriev et al. Soviet Journal of Nuclear Physics **17** (1973) 496.
26. Bychenkov V.S., Lomanov M.F., Obykhov A.I. et al. Proc. of Int. Conf. on Fifty Years with Nuclear Fission, 1989, Gaithersburg, p. 443, (1989) .
27. A.N.Smirnov, I.Yu.Gorshkov, A.V.Prokofiev et al. Proc. of 21 Int. Symp.on Nucl.Phys., Gaussig 1991, p.214 (1991)
28. A.A.Kotov, L.A.Vaishnena, V.G.Vovchenko et al. Bull.Russian Academy of Sciences - Physics, **71**, (2007) 809.
29. P.W.Lisowski, A.Gavron, W.E.Parker et al. Proc. of the NEANDC Specialists Meeting on Neutron Cross Section Standards for the Energy Region above 20 MeV, 21-23 May, 1991, Uppsala, Sweden.
30. R.Nolte, M.S.Allie, F.D.Brooks et al. Nuclear Science and Engineering **156** (2007) 197.

31. J.Rapaport, J.Ullmann, R.O.Nelson et al. Los Alamos Scientific Lab. Reports, No.11078,MS, p.1 (1987), USA
32. V.I.Goldanskiy, E.Z.Tarumov, V.S.Penkina. Doklady Akademii Nauk, Vol.101, p.1027 (1955), USSR
33. C.M.Zoeller, A.Gavron, J.P.Lestone et al. Proc. of Sem.on Fission, Habay-la-Neuve, Belgium, 1995, p.56 (1995), Belgium
34. I.V.Ryzhov, S.G.Yavshits, G.A.Tutin et al. Phys. Rev. **C83** (2011) 054603.
35. J.Katakura JAERI-Research 2003-004. JAERI, 2003.



---

Nuclear Data Section  
International Atomic Energy Agency  
Vienna International Centre, P.O. Box 100  
A-1400 Vienna  
Austria

---

e-mail: [services@iaeand.iaea.org](mailto:services@iaeand.iaea.org)  
fax: (43-1) 26007  
telephone: (43-1) 2600-21710  
Web: <http://www-nds.iaea.org>